Heat and Mass Transfer (2018) 54:1395–1403
https://doi.org/10.1007/s00231-017-2239-5

ORIGINAL

Numerical simulation of CO_2 scroll compressor in transcritical compression cycle

Hongli Wang[1] · JingRui Tian[2] · Yuanhang Du[1] · Xiujuan Hou[1]

Received: 16 September 2016 / Accepted: 20 November 2017 / Published online: 29 November 2017

Abstract

Based on the theory of thermodynamics and kinetics, the mathematical model of an orbiting scroll was established and the stress deformations were employed by ANSYS software. Under the action of pressure load, the results show that the serious displacement part is located in the center of the gear head and the maximum deformation is about 7.33 μm. The maximum radial displacement is about 4.42 μm. The maximum radial stress point occurs in the center of the gear head and the maximum stress is about 40.9 MPa. The maximum axial displacement is about 2.31 μm. The maximum axial stress point occurs in the gear head and the maximum stress is about 44.7 MPa. Under the action of temperature load, the results show that the serious deformation part is located in the center of the gear head and the maximum deformation is about 6.3 μm. The maximum thermal stress occurs in the center of the gear head and the maximum thermal stress is about 86.36 MPa. Under the combined action of temperature load and pressure load, the results show that the serious deformation part and the maximum stress are located in the center of the gear head, and the value are about 7.79 μm and 74.19 MPa, respectively.

Nomenclature

F	force (N)
h	height of vortex circle (mm)
θ	turn angle of crankshaft (rad)
P	pressure (MPa)
ρ	density (kg/m^3)
t	temperature (°C)
T	temperature (K)
θ	involute angle (rad)
α	initial angle (rad)
γ	radius of circle (mm)
Ex	elastic ratio
μ	Poisson ratio
δ	slab thickness(mm)

Subscripts

s	suction
d	exhaust
a	axial direction
t	tangential direction
r	radial direction

✉ Hongli Wang
laotingwhl@163.com

[1] College of Metallurgy and Energy, North China University of Science and Technology, Tangshan 063009, China

[2] College of Elementary Medicine, North China University of Science and Technology, Tangshan 063009, China

1 Introduction

With the growing awareness of dual threats of global warming potential and ozone depletion potential [1], people have paid more attention to the substitute of CFCs (Chlorofluorocarbons) and HCFCs (Hydro chlorofluorocarbons). Re-employ natural refrigerants are a safety choice [2]. As one of the natural refrigerant, CO_2 with zero ODP (Ozone Depletion Potential) and negligible GWP (Global Warming Potential), and it is inexpensive and friendly to environment compared with other refrigerants [3]. What is more, its volumetric refrigeration capacity is 3–10 times larger than CFC, HCFC and HFC refrigerants.

As a new type of compressor, scroll compressor was developed in the 1980s. Under the same working conditions and the same refrigerating output, the scroll compressor can reduce the volume about 40% compared with a piston compressor, and the weight reduces about 15%, but the volumetric efficiency can increases 30%, and the adiabatic efficiency increases about 10% [4]. The CO_2 scroll compressor has the characteristics of high efficiency and stable operation. Because the working process of suction, compression and exhaust proceed simultaneously, the pressure goes up with a slower speed, which the scroll compressor has a little vibration and high reliability [5].

Orbiting scroll is a main moving part of CO_2 scroll compressor and it affected by gas forces and motherboard force,

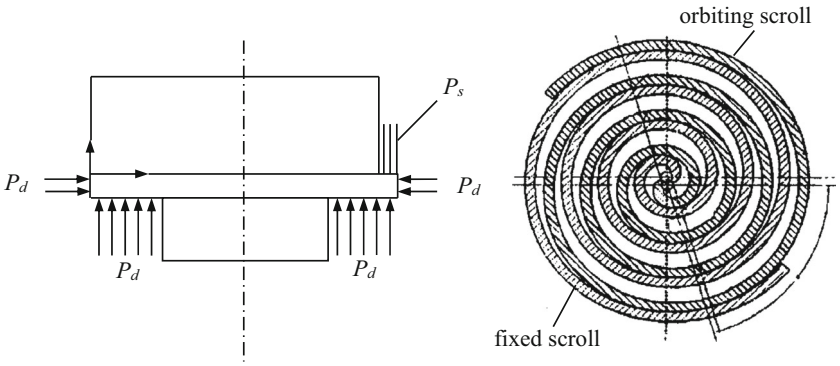

Fig. 1 Force model of CO_2 scroll compressor

which the compressor working performance and reliability are affected by the deformation. A CO_2 scroll compressor force model [6] is shown in Fig. 1. The motherboard and end plate are forced by exhaust pressure P_d, and the orbiting scroll and fixed scroll are forced by suction pressure P_s. The schematic diagram of suction process, compression process and exhaust process of a CO_2 scroll compressor were shown in Fig. 2.

Because the operation pressure and the unit volume refrigerating output of CO_2 refrigerant is higher than Freon refrigerant, the orbiting scroll size of CO_2 scroll compressor is smaller than Freon refrigerant compressor. The force on CO_2 scroll compressor orbiting scroll is more concentrated than Freon refrigerant compressor, which the design of CO_2 orbiting scroll needs higher standards. Geometric shape of orbiting scroll and fixed scroll are complex [7]. On the other hand, gear engagement position of orbiting scroll and fixed scroll are also changes, and the deformation size is micro-dimension [8]. At the same time, the rotary speed of main

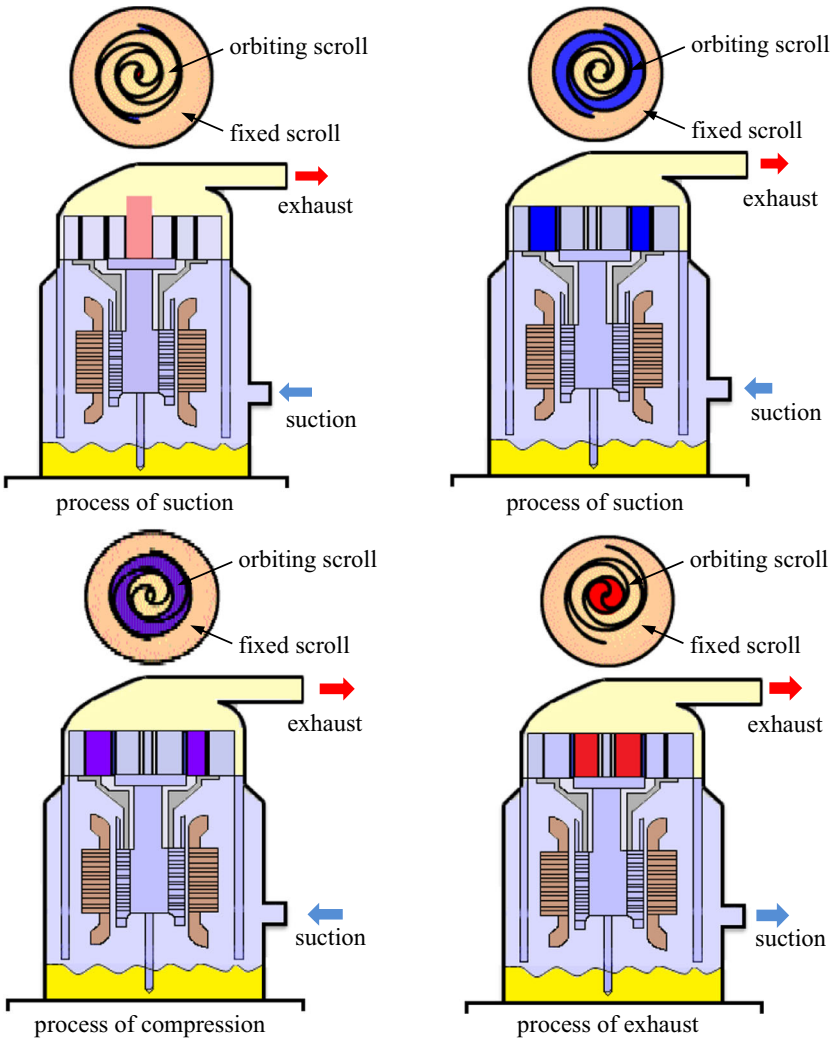

Fig. 2 Working process of CO_2 scroll compressor

Table 1 Gas forces of CO_2 scroll compressor

Parameters	Formula
axial force	$F_a = \begin{cases} \pi p_s P^2 \left[\frac{A_1}{\pi P^2}\rho_1 + \sum_{i=2}^{N}\left(2i-1-\frac{A_1}{\pi P^2}\right)\rho_i\right] & 0\le\theta\le\theta^n \\ \pi p_s P^2 \left[\frac{A_1}{\pi P^2}\rho_1 + \sum_{i=3}^{N}\left(2i-1-\frac{A_1}{\pi P^2}\right)\rho_i\right] & \theta^n\le\theta\le 2\pi \end{cases}$
radial force	$F_r = \sum_{i=1}^{N} F_{ri} = \sum_{i=1}^{N} 2ah(p_i - p_{i+1}) = 2ahp_s(p_1 - 1)$
tangential force	$F_t = \sum_{i=1}^{N} F_{ti} = p_s Ph \sum_{i=1}^{N}\left(2i-\frac{\theta}{\pi}\right)(\rho_i - \rho_{i+1})$

shaft is very high, which the test equipment is difficult to install. Therefore, the severe stress and deformation were analyzed by ANSYS finite element software, which is a kind of effective method [9].

In addition to the action of the gas force, the orbiting scroll is affected by the thermal stress. It is caused by the temperature difference of the orbiting scroll in the working process of the compressor. It is not to be ignored in the study of orbiting scroll deformation. By using the ANSYS finite element software, the thermal deformation and the distribution rule of the orbiting scroll were studied [10]. The analysis of temperature deformation and thermal stress of a scroll compressor were employed [11]. The fixed and orbiting scrolls were engaged with each other and analyses were performed to determine the stress and deformation distributions at the orbital angle where the maximum compression ratio happens.

2 Kinematics analysis of orbiting scroll and fixed scroll

Orbiting scroll and fixed scroll are the main moving part of CO_2 scroll compressor, which the kinematics analysis is the basis of strength design, reliability analysis and balance design.

The assumptions in the study are given as follows [12, 13]:

(1) Steady state operation,
(2) Negligible the heat transfer process loss of suction, compression and exhaust,
(3) Negligible the influence of gas power and gas leak,
(4) The force on the vortex circle is cantilever beam and uniformly distributed load,
(5) Negligible pressure drop of compressor,
(6) Saturated state at the compressor inlet.

Table 2 Design parameters of CO_2 scroll compressor

Parameters	Value	Parameters	Value
evaporating temperature/°C	7.2	Outlet temperature of gas cooler/°C	54.4
inlet of throttle valve/°C	46.1	Suction temperature/°C	18.3
rotary speed/r•min^{-1}	2880	Suction volume /cm^3	5.5
suction pressure/MPa	4	Discharge pressure/MPa	10

Table 3 Design parameters of CO_2 scroll compressor

Parameters	Value	Parameters	Value
theoretical refrigeration coefficient	2.27	theoretical compression work of unit mass /kJ•kg^{-1}	41.08
unit refrigerating capacity/kJ•kg^{-1}	93.33	COP	2.04
theoretical capacity of compressor /m^3•h^{-1}	0.95	actual capacity of compressor /m^3•h^{-1}	0.76
actual refrigerating capacity/kW	4.51	theoretical adiabatic indicated power /kW	1.98
actual indicated power /kW	2.32	actual input power/kW	3.49

In the work process of compressor, the gas forces changes continuously with the change of the main shaft turn angle [14]. According to different force direction, the gas forces are divided into axial force, tangential force and radial force, which were listed in Table 1.

3 Finite element model of CO_2 orbiting scroll

The design condition of CO_2 scroll compressor is referred the Chinese Standard GB/T18429–2001《fully enclosed scroll type refrigeration compressor》, and the design parameters of CO_2 scroll compressor were shown in Table 2.

According to the thermodynamic data, the design parameters of CO_2 scroll compressor were shown in Table 3.

Stress analysis of orbiting scroll was employed by involutes of circle [15]. Compares with other types of involutes,

Table 4 Basic structure parameters of CO_2 scroll compressor

Parameters	Value	Parameters	Value
radius of base circle /mm	2.28	thick-wall of scroll wrap/mm	3.00
height of vortex ring /mm	5.00	radius of gyration /mm	3.80
count of vortex ring	2.25	radius of correction circular arc /mm	6.43
initial angle /°	41.50	final deployment angle /°	14.15
pitch vortex ring /mm	12.50	connection arc radius/mm	2.55
count of scroll chamber	3	correction angle /°	120
elastic ratio / GPa	126	Poisson ratio	0.3
slab thickness/mm	12		

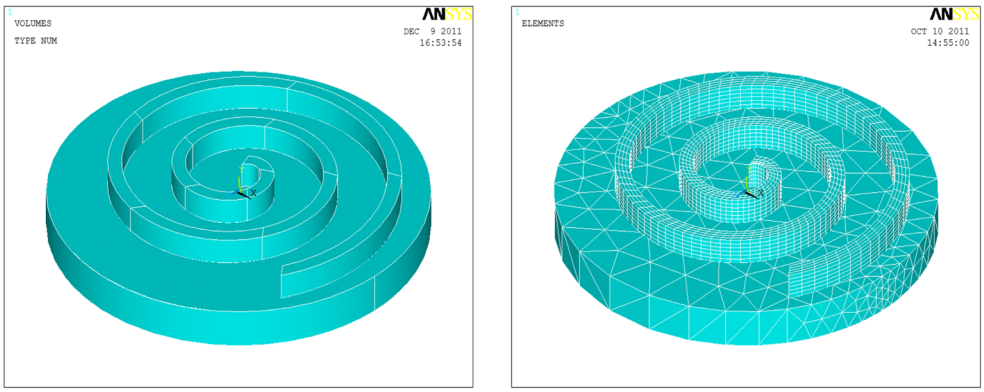

Fig. 3 Diagram of full-scale mock-up and grid division

the CO_2 scroll compressor with involutes of circles has the more compact structure and good performance [16, 17].

The inside involutes equation is [18],

$$\begin{cases} x_i = r[\cos(\varphi_i - \alpha) + \varphi_i \sin(\varphi_i - \alpha)] \\ y_i = r[\sin(\varphi_i - \alpha) - \varphi_i \cos(\varphi_i - \alpha)] \end{cases}$$

Where, φ represents the involute angle, α, denotes the initial angle of the base circle involutes.

The outside involutes equation is given by,

$$\begin{cases} x_o = r[\cos(\varphi_o - \alpha) + \varphi_o \sin(\varphi_o - \alpha)] \\ y_o = r[\sin(\varphi_o - \alpha) - \varphi_o \cos(\varphi_o - \alpha)] \end{cases}$$

The material of CO_2 orbiting scroll uses special alloy cast iron, and the elastic ratio is 126GPa, represented by *Ex*, the Poisson ratio is 0.3, represented by μ, the slab thickness is 12 mm, donated by δ. The basic structure parameters of CO_2 scroll compressor is shown in Table 4.

CO_2 transcritical cycle compressor has the characteristic of small compression ratio and big differential pressure [19]. Under the design working volume, the height of vortex ring should be reduced in order to reduce the deformation of vortex ring. On the other hand, the length of axial clearance leakage line in compression chamber is shortened by reducing the diameter of the vortex disk, and then the scroll compressor volumetric efficiency will be improved [20]. The full-scale mock-up and grid division were obtained by using the ANSYS finite element software, as shown in Fig. 3.

4 Results and discussion

According to the operating principle of scroll compressor, as well as considered the high rotary speed, the distribution of the differential pressure load along the line side was thought approximately linear. That is, in the center of the type line is exhaust pressure, and in the edge parts are suction pressure, and the middle changes continuously according to the linearity.

The pressure of CO_2 refrigerant at evaporator outlet is about 3~4 MPa, and then it into the scroll compressor. The CO_2 refrigerant is gradually compressed with rotating of scroll compressor and the gas pressure reaches as high as 10 MPa in the center of

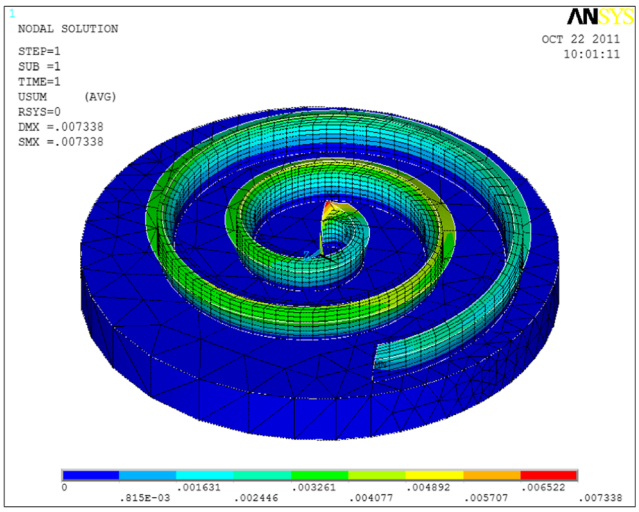

Fig. 4 Diagram of pressure load

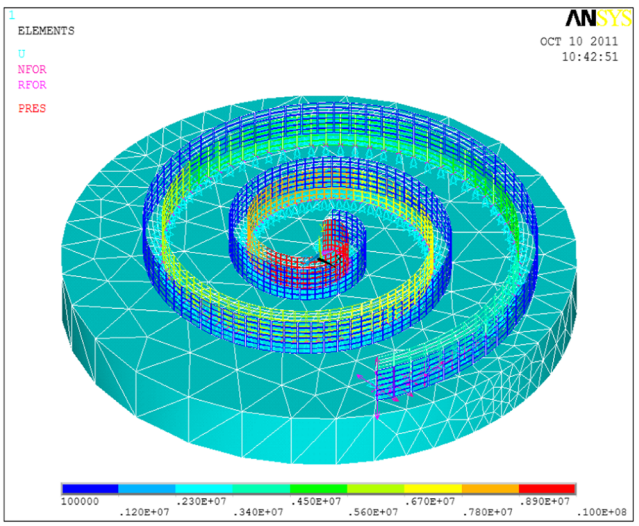

Fig. 5 Diagram of deformation variation

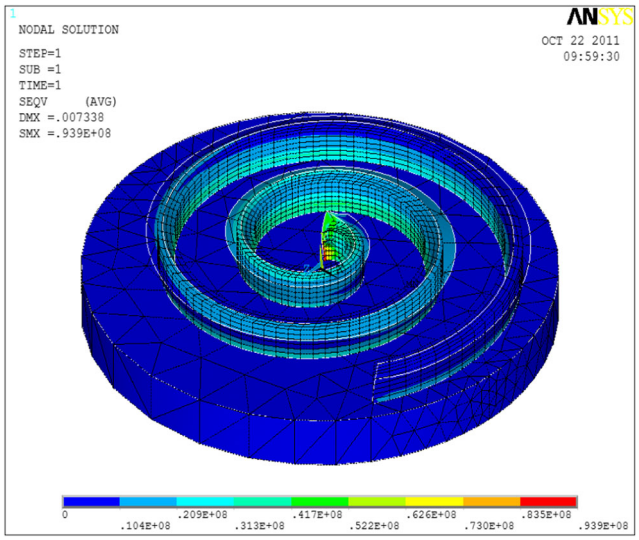

Fig. 6 Stress variation of orbiting scroll

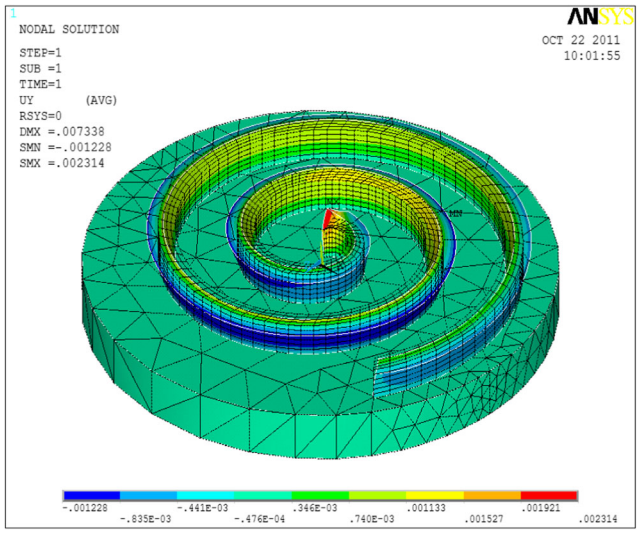

Fig. 8 Axial variation of orbiting scroll

orbiting scroll. The lateral force of the orbiting scroll is expressed by the red areas and then it changes gradually to green areas, which was shown in Fig. 4. At the same time, its outside works under the forces of relative motion by generated of orbiting scroll and fixed scroll, which was shown in blue section.

Because the exhaust orifice is located in the center of vortex disk and CO_2 refrigerant pressure reaches as high as 10 MPa. The vortex ring of orbiting scroll in the center is forced by larger gas load. From Fig. 5, in the total displacement deformation of orbiting scroll, the serious displacement part is located in the center of the dedendum, and the maximum deformation is about 7.33 μm. In addition, the displacement deformation becomes small along axial and radial of the orbiting scroll, which the minimum deformation is about 0.81 μm.

Under the gas differential pressure load as much as 6~7 MPa, which was shown in Fig. 6, the orbiting scroll internal generate greater stress and the largest stress appears in gear head, which is 93.9 MPa. The stress becomes smaller along the axial and radial, and the least stress appears in the inlet, which is about 10.4 MPa.

Radial gas forces on the vortex circle cause the vortex circle deformation from central to edge along radial direction. At the same time, the force on the vortex ring chassis will cause vortex circle migration along the radial inward.

The deformation of the orbiting scroll vortex circle includes radial deformation, axial deformation and tangential deformation. The three kinds of deformations were illustrated in Figs. 7, 8, and 9.

In Fig. 7, the radial variation of the orbiting scroll is divided into larger and smaller changes. The maximum displacement is about 4.42 μm and the minimum displacement is about 4.30 μm. In Fig. 8, the axial variation trends of the orbiting scroll likes the displacement trends. The maximum displacement deformation is located in orbiting scroll top and the

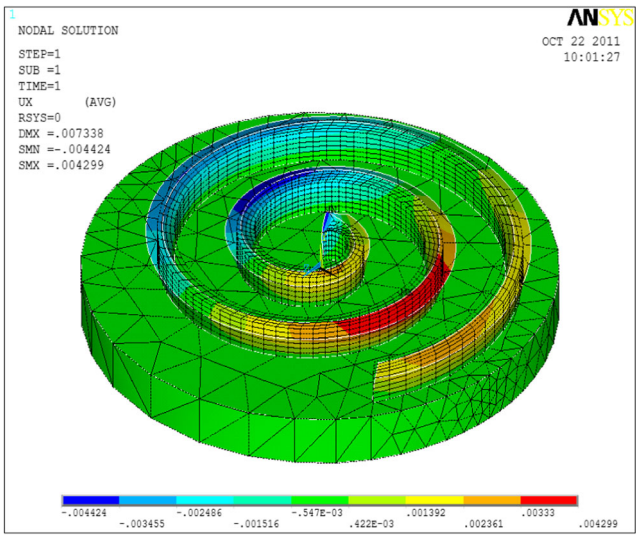

Fig. 7 Radical variation of orbiting scroll

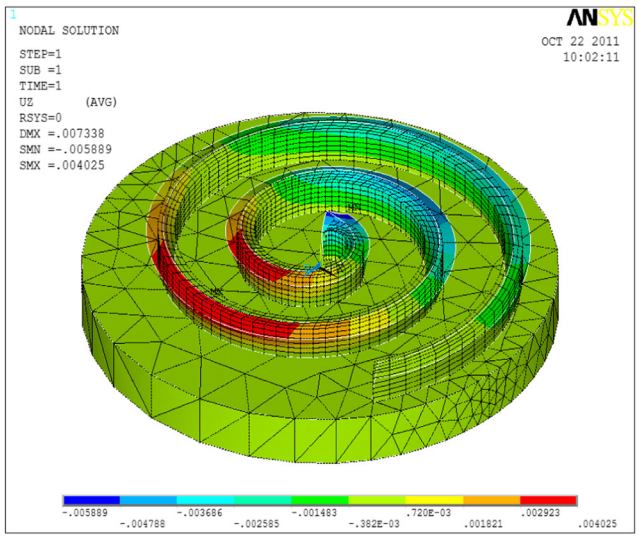

Fig. 9 Tangential variation of orbiting scroll

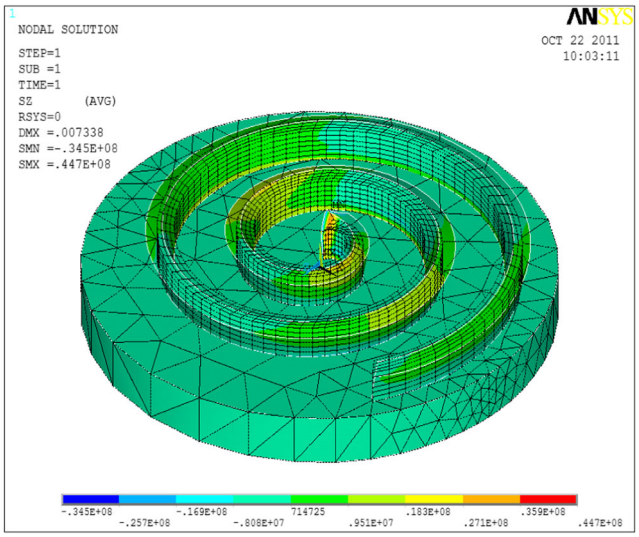

Fig. 10 Radical stress variation of orbiting scroll

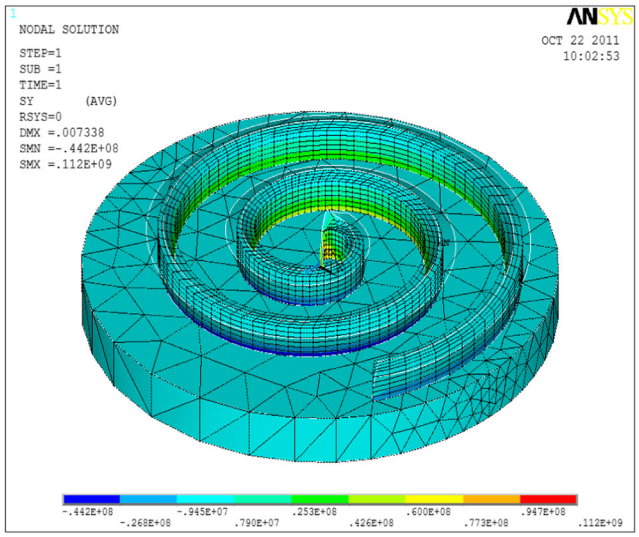

Fig. 12 Tangential stress variation of orbiting scroll

maximum displacement is about 2.31 μm. The minimum displacement is about 1.23 μm and the direction along axis to near base. The tangential variation of orbiting scroll is shown in Fig. 9. The maximum displacement is about 5.89 μm and the minimum displacement is about 4.03 μm.

It can be concluded from Figs. 7, 8, and 9 that the deformation of the orbiting scroll vortex circle is affected by the deformation of radial variation, axial variation and tangential variation. The value of axial variation is smaller than the radial and tangential changes and its role in point occurred at the gear head, so the crack and even rupture usually occurs in the gear head of vortex disk.

Figure 10 shows the radical stress variation of the orbiting scroll. The stress decreases gradually along the radial direction from the center to edge. The maximum stress point occurs in the center of the gear head and the maximum stress is about 40.9 MPa. The minimum stress occurs in the inlet and the value is about 18.2 MPa. Radial deformation is mainly due to the results of the orbiting scroll radial gas forces.

The axial stress variation of orbiting scroll was depicted in Fig. 11. The stress decreases gradually along the axial direction from gear head to dedendum. The maximum stress point occurs in the gear head and the maximum stress is about 44.7 MPa. The minimum stress occurs in the inlet and the value is about 34.5 MPa. The axial force can cause the axis to distort, and causes the orbiting scroll and the fixed scroll to separate each other, and then increases the axial clearance, thus the axial leakage loss of CO_2 refrigerate increases.

Figure 12 shows the tangential stress variation of the orbiting scroll. The stress decreases gradually along the tangential direction from the center to edge. The maximum stress point occurs in dedendum of the vortex circle and the maximum stress is about 112.0 MPa. The minimum stress occurs in edge of the vortex circle and the value is about 44.2 MPa.

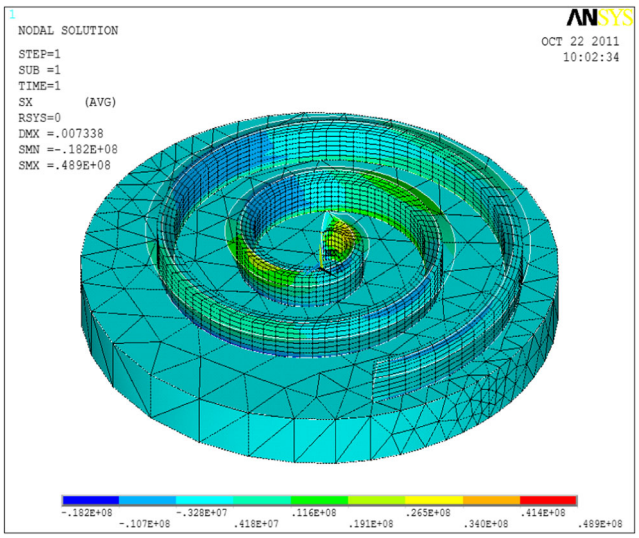

Fig. 11 Axial stress variation of orbiting scroll

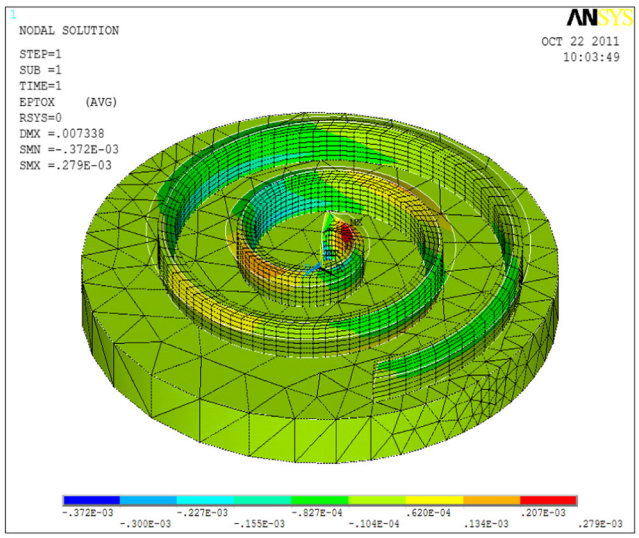

Fig. 13 Axial strain variation of orbiting scroll

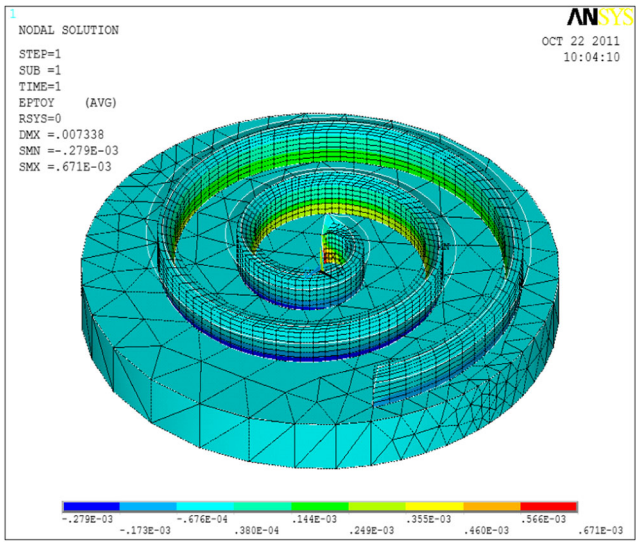

Fig. 14 Strain radical variation of orbiting scroll

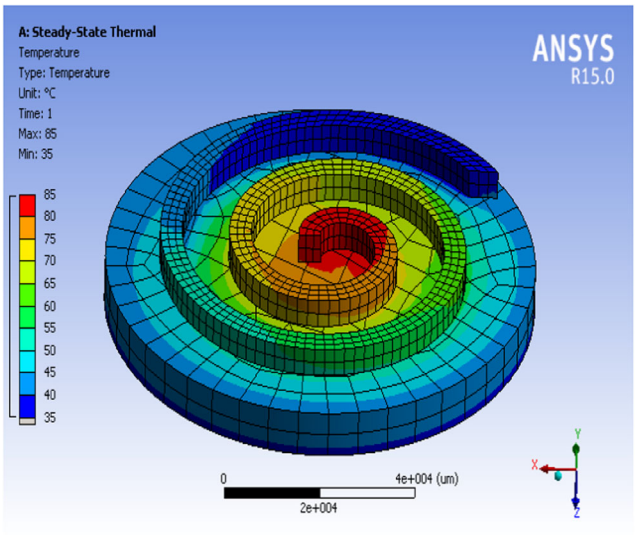

Fig. 16 Temperature distribution of orbiting scroll

From Figs. 10, 11, and 12, the analysis indicated that the tangential stress variation of the orbiting scroll has the biggest value among the three kinds of stress variations, and it occurs in dedendum of the vortex circle. So the parts of dedendum can be easily to cause the distortion and even damage [21].

Figure 13 presents the axial strain variation of orbiting scroll and the distribution has the characteristic of symmetry. The axial variation decrease gradually along axial direction from the center to the edge and the largest strain variation occurs in the gear head of vortex circle, which the maximum strain variation is about 3.72 μm. In the area of not change significantly, axial strain reduces gradually along the axial direction from left to right, and the minimum strain in the central of vortex circle, which the minimum strain variation is about 2.79 μm.

The radical strain variation mainly happened in the bottom of orbiting scroll vortex circle, as shown in Fig. 14. The biggest strain appears in dedendum of vortex circle and the maximum strain variation is about 6.71 μm. Along the radial direction from the center to edge, the strain becomes smaller gradually and the minimum stress points in the edge of vortex circle, and the value is about 2.79 μm.

The trend of tangential strain is similar with the axial strain, which is shown in Fig. 15. The biggest strain in the gear head and the maximum strain variation is about 2.78 μm. Along the radial direction from the center to edge, the strain becomes smaller gradually and the minimum stress appears in the central part of the each vortex, and the value is about 2.40 μm.

From Fig. 13 to Fig. 15, the analysis showed that the radical strain variation occurs in dedendum of vortex circle and the maximum strain variation is about 6.71 μm. The maximum

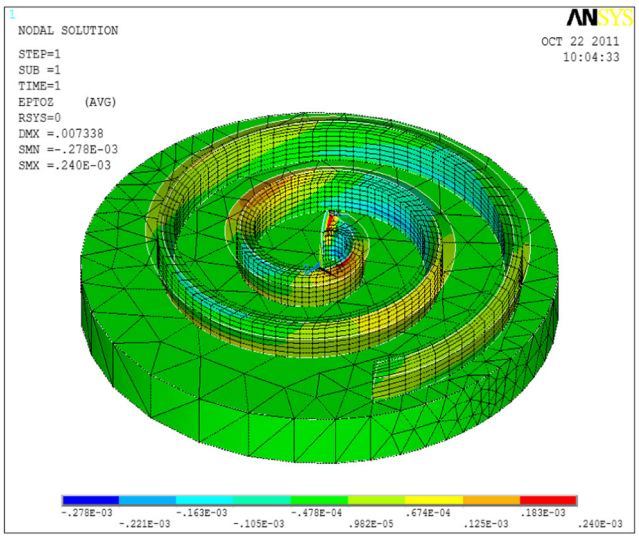

Fig. 15 Strain tangential variation of orbiting scroll

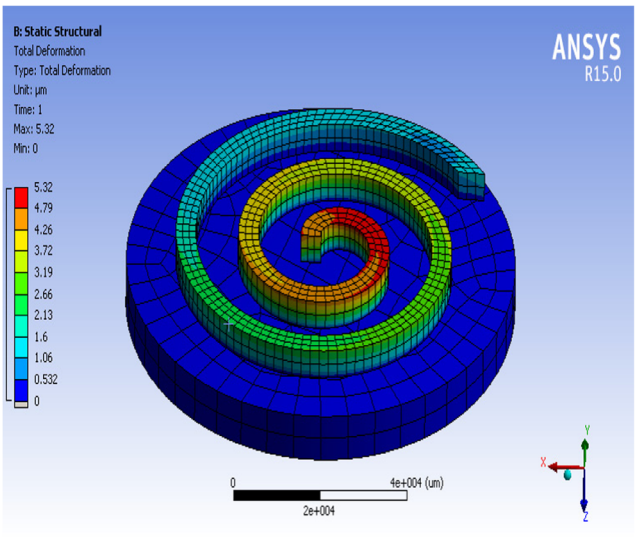

Fig. 17 Thermal deformation of orbiting scroll

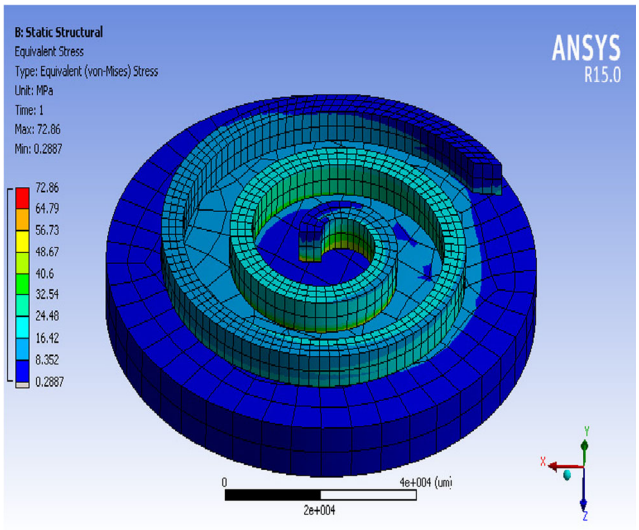

Fig. 18 Thermal stress of orbiting scroll

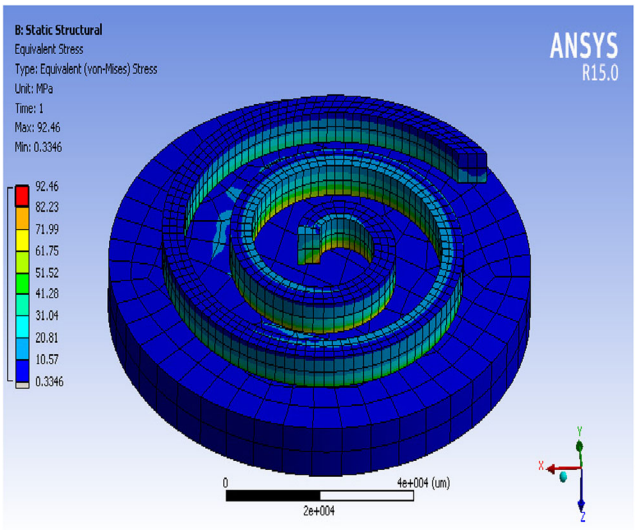

Fig. 20 Coupled stress of orbiting scroll in pressure and temperature

strain variation of axial strain variation and tangential strain variation occur in the gear head of orbiting scroll and easily lead to the crack and even rupture usually.

In order to simulate the temperature distribution of the orbiting scroll in the actual working process, the temperature load is applied to the temperature field along the direction of the orbiting scroll. The highest temperature is 85 °C and the lowest temperature is 35 °C. On the back of the chassis of linearly decreasing along radius direction change of temperature field, the center temperature is 85°Cand the boundary temperature is 35 °C, as shown in Fig. 16.

With orbiting scroll rotating, the CO2 refrigerant is gradually compressed, and the center temperature can reach to 85 °C and above. The temperature distributions of the orbiting scroll and the CO2 refrigerant have the same rule. So the temperature distribution along orbiting scroll can be seen by the gas between the entrances to the green into red gas exports.

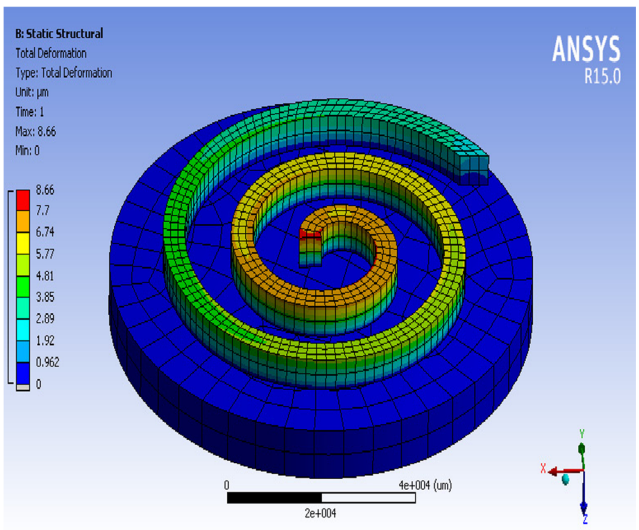

Fig. 19 Coupled deformation of orbiting scroll in pressure and temperature

Under the temperature difference load as much as 35 °C~85 °C, the thermal stress deformation of orbiting scroll is shown in Fig. 17. Due to the discharge temperature of the CO_2 refrigerant at the center of the orbiting scroll has up to 85 °C, there has the maximum temperature load and thermal stress deformation. The maximum thermal stress deformation is about 6.3 μm and the minimum deformation is 0.7 μm.

Figure 18 presents the thermal stress of orbiting scroll under the given temperature difference load. It can be seen that the maximum thermal stress occurs in gear root and the maximum stress is about 86.36 MPa. The amount of thermal stress gradually decreases along the radial and axial, and the minimum value is 9.95 MPa.

The coupled deformation of orbiting scroll in pressure and temperature were simulated, as shown in Fig. 19. It can be seen that the maximum deformation occurs in gear root and the maximum value is about 7.79 μm. The amount of deformation gradually decreases along the radial and axial, and the minimum deformation is 0.86 μm.

The coupled stress of orbiting scroll in pressure and temperature were also simulated, as shown in Fig. 20. Under different temperature and gas pressure, the orbiting scroll has different stress and the maximum stress occurs in gear root, which the maximum value is 74.19 MPa. The amount of stress gradually decreases along the radial and axial, and the minimum value is 8.6 MPa.

From Figs. 19 and 20, there are the maximum deformation and maximum stress in orbiting scroll gear root. Because of big differential pressure of CO_2 transcritical compressor, the orbiting scroll withstands a bigger force than Freon refrigerant compressor. As a result, the orbiting scroll is more likely to wear and then damaged.

5 Conclusions

The stress deformation and thermal distribution of the orbiting scroll of a scroll compressor were employed by the ANSYS finite element software. Some fundamental data were obtained for improving the performance of the CO_2 transcritical cycle and then developing prototype products. The conclusions in the study are given as follows.

(1) Under the action of gas load separately, the serious displacement part is located in the center of the gear head and the maximum deformation is about 7.33 μm. The maximum radical displacement of orbiting scroll is about 4.42 μm and the minimum displacement is about 4.30 μm. The maximum radical stress point occurs in the center of the gear head and the maximum stress is about 40.9 MPa and the minimum stress is about 18.2 MPa.
(2) The maximum axial displacement is about 2.31 μm and the minimum displacement is about 1.23 μm. The maximum axial stress point occurs in the gear head and the maximum stress is about 44.7 MPa. The minimum stress occurs in the inlet and the value is about 34.5 MPa.The maximal tangential displacement is about 5.89 μm and the minimum displacement is about 4.03 μm. The maximum tangential stress is about 112.0 MPa and the minimum stress is about 44.2 MPa.
(3) Under the action of temperature load separately, the maximum deformation is about 6.3 μm and the minimum deformation is about 0.7 μm. The maximum thermal stress occurs in the center of the gear head and the maximum value is about 86.36 MPa, and the minimum value is about 9.95 MPa.
(4) Under the coupling action of the temperature and pressure, the serious deformation part is located in the center of the gear head and the maximum deformation is about 7.79 μm, the minimum deformation is about 0.86 μm. The maximum stress occurs in the center of the gear head and the maximum stress is about 74.19 MPa, and the minimum stress is about 8.6 MPa.

Acknowledgements The authors acknowledge the support by the natural science foundation of Hebei Province (E2015209239), the support by the Science and technology project of Hebei Province (15214317) and the support of North China University of Science and Technology Fund (SP201306).

References

1. CALM JM (2007) Resource ozone and global warming implications of refrigerant selection for large chillers, In: Proceedings of the 22nd international congress of refrigeration, Beijing, pp 1–9
2. Hirao T, Mizukami H, Takeuchi M, et al. (2000) Development of air conditioning system using CO_2 for automobile. In: The proceedings of the 4th IIR-Gustav Lorentzen conference on natural working fluids, Purdue University, pp. 193–200
3. Brown JS, Yana-Motta SF, Domanski PA (2002) Comparitive analysis of an automotive air conditioning systems operating with CO_2 and R134a. Int J Refrig 25(1):19–32
4. Cuevas C, Lebrun J, Lemort V, Winandy E (2010) Characterization of a scroll compressor under extended operating conditions. Appl Therm Eng 30(6–7):605–615
5. Sánchez D, Torrella E, Cabello R, Llopis R (2010) Influence of the superheat associated to a semihermetic compressor of a transcritical CO_2 refrigeration plant. Appl Therm Eng 30(4):302–309
6. Liu Y, Hung C, Chang Y (2009) Mathematical model of bypass behaviors used in scroll compressor. Appl Therm Eng 29(5–6): 1058–1066
7. Blunier B, Cirrincione G, Hervé Y, Miraoui A (2009) A new analytical and dynamical model of a scroll compressor with experimental validation. Int J Refrig 32(5):874–891
8. Evandro LL, Pereira, Cesar J, Deschamps (2017) A heat transfer correlation for the suction and compression chambers of scroll compressors. Int J Refrig 82:325–334
9. Becerra JA, Jimenez FJ, Torres M, Sanchez DT, Carvajal E (2011) Failure analysis of reciprocating compressor crankshafts. Eng Fail Anal 18(2):735–746
10. Lin C, Chang Y, Liang K et al (2005) Temperature and thermal deformation analysis on scrolls of scroll compressor [J]. Appl Therm Eng 25:1724–1739
11. Jang K, Jeong S (2006) Experimental investigation on convective heat transfer mechanism in a scroll compressor. Int J Refrig 29(5):744–753
12. Yang JL, Ma YT, Li MX, Guan HQ (2005) Exergy analysis of transcritical carbon dioxide refrigeration cycle with an expander. Energy 30(7):1162–1175
13. Hyun JK, Jong MA, Sung OC (2008) Numerical simulation on scroll expander-compressor unit for CO_2 trans-critical cycles. Appl Therm Eng 28(13):1654–1661
14. Witek L (2011) Numerical stress and crack initiation analysis of the compressor blades after foreign object damage subjected to high-cycle fatigue. Eng Fail Anal 18(8):2111–2125
15. Liu Y, Hung C, Chang Y (2010) Study on involute of circle with variable radii in a scroll compressor. Mech Mach Theory 45(11): 1520–1536
16. Chen Y-C, Liu C-C (2011) Contact stress analysis of concave conical involute gear pairs with non-parallel axes. Finite Elem Anal Des 47(4):443–452
17. Ziatdinov R, Yoshida N, Kim T-w (2012) Analytic parametric equations of log-aesthetic curves in terms of incomplete gamma functions. Comput Aided Geom Des 29(2):129–140
18. Wang B, Shi W, Li X, Yan Q (2008) Numerical research on the scroll compressor with refrigeration injection. Appl Therm Eng 28(5–6):440–449
19. Wang H, Ma Y, Tian J, Li M (2011) Theoretical analysis and experimental research on transcritical CO_2 two stage compression cycle with two gas coolers (TSCC+TG) and the cycle with intercooler (TSCC+IC). Energy Convers Manag 52(8–9):2819–2828
20. Park YC, Kim Y, Cho H (2002) Thermodynamic analysis on the performance of a variable speed scroll compressor with refrigerant injection. Int J Refrig 25(8):1072–1082
21. Lee S-J, Kim H-B, Huh J-K, Lee S-J, Ahn B-H (2003) Quantitative analysis of flow inside the accumulator of a rotary compressor. Int J Refrig 26(3):321–327